

Optimization design of fragment-type microstrip filter using boundary-based filtering operator

Wa Kong¹, Da-Wei Ding^{1a)}, Jing Xia^{1,2}, Xiao-Dong Ding¹,
and Li-Xia Yang¹

¹ School of Computer Science and Communication Engineering, Jiangsu University,
Zhenjiang 212013, China

² State Key Laboratory of Millimeter Waves, Southeast University,
Nanjing 210096, China

a) dingdawei@ujs.edu.cn

Abstract: A novel optimization design method using boundary-based weighted sum filtering operator is proposed for microstrip filter design. The proposed operator is combined with multiobjective evolutionary algorithm based on decomposition combined with enhanced genetic operators and two-dimensional median filtering operator (MOEA/D-GO-II), which can maintain the population diversity and obtain wider rejection bandwidth. For verification, it is used to design fragment-type microstrip band-stop filter for rejecting one of the fifth generation (5G) bands, 3.3 GHz–3.6 GHz. Both simulated and measured results verified the expected responses of the design. Comparison result shows that more alternative designs could be obtained using the proposed method.

Keywords: boundary-based filtering operator, band-stop filter, fragment-type, optimization

Classification: Microwave and millimeter-wave devices, circuits, and modules

References

- [1] J. S. Hong and M. J. Lancaster: *Microstrip Filters for RF/Microwave Applications* (Wiley, New York, 2001).
- [2] M. Yang, *et al.*: “A novel open-loop DGS for compact bandstop filter with improved Q factor,” ISAPE (2008) 649 (DOI: [10.1109/ISAPE.2008.4735297](https://doi.org/10.1109/ISAPE.2008.4735297)).
- [3] S. U. Rehman, *et al.*: “Compact bandstop filter using defected ground structure (DGS),” SIEPCPC (2011) 1 (DOI: [10.1109/SIEPCPC.2011.5876972](https://doi.org/10.1109/SIEPCPC.2011.5876972)).
- [4] J.-S. Lim, *et al.*: “A vertically periodic defected ground structure and its application in reducing the size of microwave circuits,” IEEE Microw. Wireless Compon. Lett. **12** (2002) 479 (DOI: [10.1109/LMWC.2002.805941](https://doi.org/10.1109/LMWC.2002.805941)).
- [5] L. Chen, *et al.*: “Novel W-slot DGS for band-stop filter,” ISAP (2013) 981.
- [6] J. Garcia-Garcia, *et al.*: “Microwave filters with improved stopband based on subwavelength resonators,” IEEE Trans. Microw. Theory Techn. **53** (2005) 1997 (DOI: [10.1109/TMTT.2005.848828](https://doi.org/10.1109/TMTT.2005.848828)).

- [7] J. Zhang, *et al.*: “A harmonic suppressed Wilkinson power divider using complementary split ring resonator,” *J. Electromagn. Waves Appl.* **21** (2007) 811 (DOI: [10.1163/156939307780749165](https://doi.org/10.1163/156939307780749165)).
- [8] M. Gil, *et al.*: “Composite right/left-handed material transmission lines based on complementary split ring resonators and their applications to very wide band and compact filter design,” *IEEE Trans. Microw. Theory Techn.* **55** (2007) 1296 (DOI: [10.1109/TMTT.2007.897755](https://doi.org/10.1109/TMTT.2007.897755)).
- [9] S. S. Karthikeyan and R. S. Kshetrimayum: “Performance enhancement of microstrip bandpass filter using CSSRR,” *ACT* (2009) 67 (DOI: [10.1109/ACT.2009.27](https://doi.org/10.1109/ACT.2009.27)).
- [10] F. Aznar-Ballesta, *et al.*: “Recursive active filter with metamaterial unequal Wilkinson power dividers,” *EuMC* (2010) 930 (DOI: [10.23919/EUMC.2010.5616054](https://doi.org/10.23919/EUMC.2010.5616054)).
- [11] Q. Zhao, *et al.*: “Compact microstrip bandpass filter with fragment-loaded resonators,” *Microw. Opt. Technol. Lett.* **56** (2014) 2896 (DOI: [10.1002/mop.28726](https://doi.org/10.1002/mop.28726)).
- [12] D. Ding, *et al.*: “High-efficiency scheme and optimization technique for design of fragment-type isolation structure between multiple-input and multiple-output antenna,” *IET Microw. Antennas Propag.* **9** (2015) 933 (DOI: [10.1049/iet-map.2014.0742](https://doi.org/10.1049/iet-map.2014.0742)).

1 Introduction

Band-stop filters are widely used in wireless communication systems to reject unwanted signals. In the past years, many structures have been proposed to realize microstrip band-stop filters with compact size and high performance, where the high performance often refers to wide stop-band bandwidth, good stop-band return loss, low pass-band insertion loss, sharp out-of-band rejection, and spurious modes suppression [1, 2, 3, 4, 5, 6]. In [1], open stub is used to design microstrip band-stop filter. However, the rejection bandwidth is very narrow. Many structures, such as electromagnetic band gap (EBG) [2, 3] and defected ground structure (DGS) [4, 5], have been proposed to improve stop-band bandwidth. In addition, split ring resonator (SRR), complimentary SRR (CSRR), and composite right/left-handed metamaterial transmission line structure are also used for miniaturization and high performance requirements [6, 7, 8, 9, 10].

Recently, fragment-type microstrip structure attracts more and more attention due to its compactness and spurious modes suppression [11, 12]. As shown in Fig. 1, the fragment-type structure could be described by gridding a designated area through assigning with “1” or “0”, where cells “1” are to be metalized and cells “0” are to be non-metalized. Then a two-dimensional “0/1” matrix corresponding to the fragment-type structure is optimized by using multiobjective evolutionary algorithm based on decomposition combined with enhanced genetic operators (MOEA/D-GO) [11]. In order to obtain the fragment-type structures with low overall loss, two-dimensional (2D) median filtering operator is introduced to MOEA/D-GO, called MOEA/D-GO-II [12].

However, MOEA/D-GO-II converges fast at the expense of population diversity, which might make the algorithm converge to local optimal or reduce the

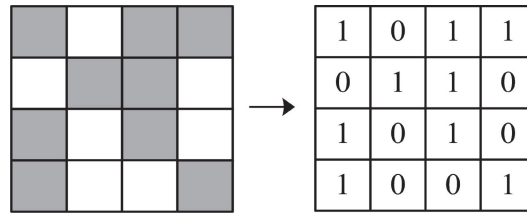


Fig. 1. Fragment-type structure and its design matrix.

number of alternative designs. In order to overcome this problem, boundary-based filtering operator, metalizing the edge cell when it is bounded by metal and non-metalizing the edge cell when it is bounded by air, is proposed in this paper. Boundary-based filtering operator has more possibility to maintain the connectivity of the boundary of the metal conductor, thus more metalized cells are remained to maintain the population diversity, and it is beneficial for trapping the current into the isolation structure through conductor to obtain perfect return loss and isolation, thus obtain wider rejection bandwidth. For verification, a fragment-type microstrip band-stop filter with rejection bandwidth of 3.3 GHz–3.6 GHz was simulated and measured.

2 Boundary-based filtering operator

Boundary-based filtering operator is proposed at first. Fig. 2(a) shows the original fragment-type structure and its boundary conditions, along with their 0/1 design matrix. Fig. 2(b)–(c) illustrate the obtained fragment-type structures through different filtering operators, along with their filtering matrices (FM). In these filtering operators, each cell is assigned with “1” or “0” according to the following equation,

$$H(i, j) = \begin{cases} 1 & \left(\text{if } d(i, j) \geq \frac{|FM|}{2} \right) \\ 0 & \text{(otherwise)} \end{cases} \quad (1)$$

$$d(i, j) = \sum_{m=-1}^1 \sum_{n=-1}^1 H(i+m, j+n) \times FM(m, n)$$

$$(i = 1, 2, \dots, M; j = 1, 2, \dots, N)$$

where $|FM|$ represents the sum of all elements of the FM, $M \times N$ defines the size of the design matrix, and $H(i+m, j+n)$ denotes the value of the neighborhood of each cell [12].

From Fig. 2, it is clearly seen that boundary-based filtering operators determine the matrix H considering the boundary. It should be noted that weighted sum filtering weakens the role of its diagonal sister when compared to original median filtering. From Fig. 2, it is also obviously observed that the edge (region A) of the fragment-type structure maintains the connectivity of the boundary, and the overall metalized cells assigned with “1” is more than that generated by the original median filtering operator, which is consistent with the descriptions in introduction.

In Fig. 3, the proposed boundary-based filtering operator is combined with MOEA/D-GO-II. The framework employs the boundary-based filtering operator after genetic operators to maintain the connectivity of the boundary of the metal

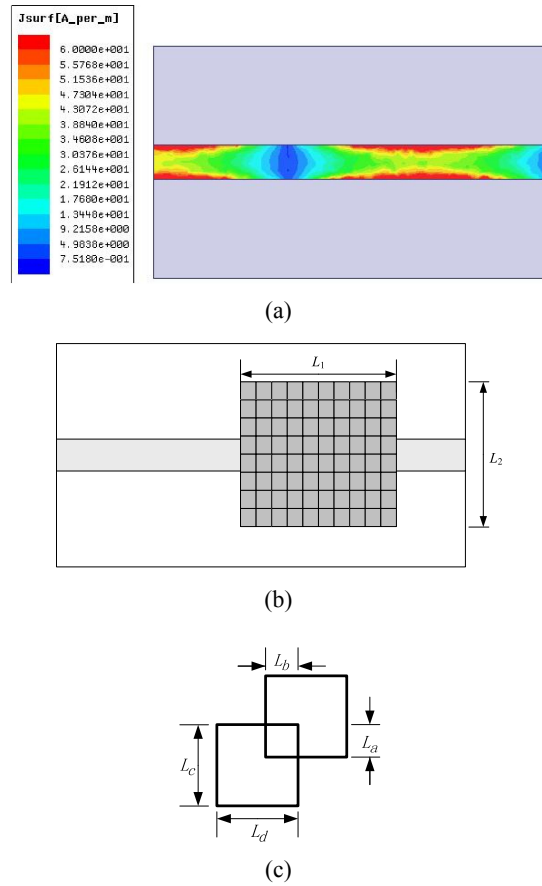


Fig. 4. Configuration of fragment-type microstrip filter.

conductor, thus more metalized cells are remained to maintain the population diversity.

3 Microstrip band-stop filter design

3.1 Design results

In order to obtain band-stop filter design rejecting 3.3 GHz–3.6 GHz, the following objective functions are considered.

$$F_1 = \frac{10}{\min_{\omega \in [1\text{GHz}, \omega_1] \cup [\omega_2, 6\text{GHz}]} |S_{11}(\omega)|_{\text{dB}}}, \quad (2)$$

$$F_2 = \max_{\omega \in [1\text{GHz}, \omega_1] \cup [\omega_2, 6\text{GHz}]} |S_{21}(\text{dB})|, \quad (3)$$

$$F_3 = \frac{20}{\min_{\omega \in [3.3\text{GHz}, 3.6\text{GHz}]} |S_{21}(\omega)|_{\text{dB}}}, \quad (4)$$

where $|S_{11}(\omega)|_{\text{dB}}$ represents return loss in dB, $|S_{21}(\omega)|_{\text{dB}}$ represents insertion loss in dB, the constants in (2)–(4) is used for normalization, ω_1 is set as 3.0 GHz, and ω_2 is set as 4.0 GHz. It's obviously seen that when F_i ($i = 1, 2, 3$) is smaller than 1, the return loss in pass-band is less than 10-dB, the insertion loss in pass-band is less than 1-dB, and the rejection over 3.3 GHz–3.6 GHz is more than 20-dB.

In this paper, a $50\ \Omega$ microstrip transmission line with width of 3.05 mm is considered as shown in Fig. 4, which is printed on a FR4 substrate ($20.4\ \text{mm} \times 35\ \text{mm} \times 1.6\ \text{mm}$) with relative dielectric constant of 4.4. Fig. 4(a)

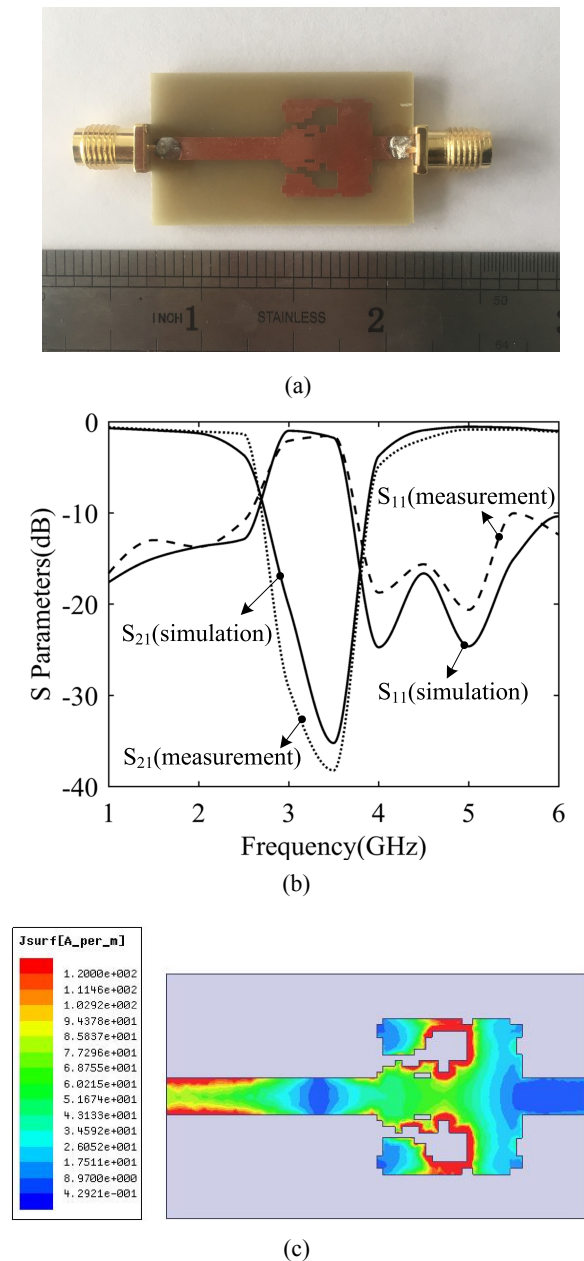


Fig. 5. The optimized fragment-type microstrip band-stop filter. (a) photograph of the fabricated filter, and (b) simulation and measurement results, and (c) current distribution at 3.45 GHz.

illustrates the current distribution at 3.45 GHz, where the region with the largest current intensity is loaded with fragment-type structure. In this paper, the fragment-type structure covers a design space of $12.1 \text{ mm} \times 13.05 \text{ mm}$ (i.e. $L_1 \times L_2$) which could be divided into 22×24 cells. For each metallic element, both L_c and L_d are set as 0.6 mm, and they overlap for electrical contact ($L_a = L_b = 0.1 \text{ mm}$).

The optimization kernel is constructed through combining boundary-based MOEA/D-GO-II with ANSYS HFSS 13.0 [11, 12]. Boundary-based MOEA/D-GO-II is implemented by using Visual C++ 6.0 and HFSS is controlled automatically by VBScript. After 35 iterations, 8 designs are obtained. One of them is fabricated and tested, as shown in Fig. 5(a).

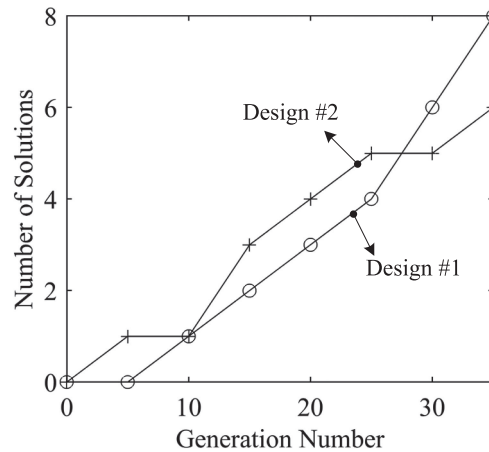


Fig. 6. The number of solutions against iteration number.

From Fig. 5(b), good agreement between simulated and measured return loss can be observed. Measured results clearly show that, over 3.3 GHz–3.6 GHz, the insertion loss is less than 20-dB and the return loss is less than 2-dB. For the pass-band, the return loss is less than 10-dB. The slight difference between the simulated and measured results is believed to be caused by the fabrication and measurement error. Fig. 5(c) illustrates that the current at 3.45 GHz could be effectively trapped in the fragment-type structure, which leads to the bandwidth rejection.

3.2 Comparison of the optimization methods

In this section, comparison on the number of obtained alternative designs through boundary-based MOEA/D-GO-II and original MOEA/D-GO-II is conducted. For demonstration, these two design processes are denoted as design #1 and design #2, respectively. Fig. 6 gives the number of obtained alternative designs against iteration number. From Fig. 6, it's found that, after 30 iterations, the boundary-based MOEA/D-GO-II can generate more number of satisfied solutions, which accords with the expectation. Therefore, it's concluded that boundary-based filtering operator is promising for obtaining more alternative designs.

4 Conclusions

In this paper, a novel boundary-based weighted sum filtering operator is proposed for fragment-type structure designs. A microstrip band-stop filter rejecting 3.3 GHz–3.6 GHz is designed through the proposed operator combined with MOEA/D-GO-II. Comparison on the number of obtained designs shows that more alternative designs could be generated, which has great potential in engineering applications.

Acknowledgments

This work was supported by the National Science Foundation of China under Grant No. 61701199 and the National Natural Science Foundation of the Jiangsu Higher Education Institutions of China Grant No. 16KJB510006. This work was also supported by the Natural Science Foundation of Jiangsu Province of China under Grant No. BK20150528.